

Effect of rapid thermal annealing on Mg x Zn 1 – x O films prepared by radio-frequency magnetron sputtering

Kuang-Po Hsueh, Chun-Ju Tun, Hsien-Chin Chiu, Yu-Ping Huang, and Gou-Chung Chi

Citation: *Journal of Vacuum Science & Technology B* **28**, 720 (2010); doi: 10.1116/1.3442476

View online: <http://dx.doi.org/10.1116/1.3442476>

View Table of Contents: <http://scitation.aip.org/content/avs/journal/jvstb/28/4?ver=pdfcov>

Published by the AVS: Science & Technology of Materials, Interfaces, and Processing

Articles you may be interested in

Effects of rapid thermal annealing on properties of Ga-doped Mg_xZn_{1-x}O films and Ga-doped Mg_xZn_{1-x}O/AlGa_N heterojunction diodes

J. Appl. Phys. **116**, 063501 (2014); 10.1063/1.4892591

A comparative study of electronic and structural properties of polycrystalline and epitaxial magnetron-sputtered ZnO:Al and Zn_{1-x}Mg_xO:Al Films—Origin of the grain barrier traps

J. Appl. Phys. **114**, 063709 (2013); 10.1063/1.4817376

High-temperature stability of postgrowth-annealed Al-doped Mg_xZn_{1-x}O films without the phase separation effect


J. Vac. Sci. Technol. B **30**, 061201 (2012); 10.1116/1.4754813

Radio-frequency superimposed direct current magnetron sputtered Ga:ZnO transparent conducting thin films





J. Appl. Phys. **111**, 093718 (2012); 10.1063/1.4709753

Hydrogen-doped high conductivity ZnO films deposited by radio-frequency magnetron sputtering

Appl. Phys. Lett. **85**, 5628 (2004); 10.1063/1.1835991



Instruments for Advanced Science

<p>Contact Hiden Analytical for further details: W www.HidenAnalytical.com E info@hiden.co.uk CLICK TO VIEW our product catalogue</p>	 <p>Gas Analysis</p> <ul style="list-style-type: none"> › dynamic measurement of reaction gas streams › catalysis and thermal analysis › molecular beam studies › dissolved species probes › fermentation, environmental and ecological studies 	 <p>Surface Science</p> <ul style="list-style-type: none"> › UHV TPD › SIMS › end point detection in ion beam etch › elemental imaging - surface mapping 	 <p>Plasma Diagnostics</p> <ul style="list-style-type: none"> › plasma source characterization › etch and deposition process reaction › kinetic studies › analysis of neutral and radical species 	 <p>Vacuum Analysis</p> <ul style="list-style-type: none"> › partial pressure measurement and control of process gases › reactive sputter process control › vacuum diagnostics › vacuum coating process monitoring
---	--	--	--	--

Effect of rapid thermal annealing on $\text{Mg}_x\text{Zn}_{1-x}\text{O}$ films prepared by radio-frequency magnetron sputtering

Kuang-Po Hsueh^{a)}

Department of Electronics Engineering, Vanung University, Chung-Li 32061, Taiwan

Chun-Ju Tun

National Synchrotron Radiation Research Center, Hsinchu 30076, Taiwan

Hsien-Chin Chiu

Department of Electronics Engineering, Chang Gung University, Tao-Yuan 33302, Taiwan

Yu-Ping Huang and Gou-Chung Chi

Department of Photonics, National Chiao Tung University, Hsinchu 30010, Taiwan

(Received 19 January 2010; accepted 10 May 2010; published 1 July 2010)

This study investigates the effects of thermal annealing on the $\text{Mg}_x\text{Zn}_{1-x}\text{O}$ films. $\text{Mg}_x\text{Zn}_{1-x}\text{O}$ films were deposited by a radio-frequency magnetron sputtering system using a 6 in. ZnO/MgO (80/20 wt %) target. The Hall results, x-ray diffraction (XRD), transmittance, and x-ray photoelectron spectroscopy (XPS) were measured. The XRD results indicate that the appearance of only (111) peaks in the as-grown $\text{Mg}_x\text{Zn}_{1-x}\text{O}$ film is a sign of the cubic single phase, whereas the appearance of ZnO (002) peaks in $\text{Mg}_x\text{Zn}_{1-x}\text{O}$ films annealed at 700 and 800 °C confirms the formation of a wurtzite single-phase crystal. The existence of a weak (002)-wurtzite peak besides the (111)-cubic peak indicates the coexistence of two phases. The absorption spectra of $\text{Mg}_x\text{Zn}_{1-x}\text{O}$ annealed at 700 and 800 °C show two stages at wavelengths of 357 and 261 nm. The XPS spectra of $\text{Mg}_x\text{Zn}_{1-x}\text{O}$ films were also demonstrated. The results of this study show that the ZnO films were separated from $\text{Mg}_x\text{Zn}_{1-x}\text{O}$ films after higher thermal annealing. © 2010 American Vacuum Society. [DOI: 10.1116/1.3442476]

I. INTRODUCTION

Zinc oxide (ZnO) transparent conductive oxide (TCO) is a well-known wide-band-gap material, and can be used to form transparent contact layers in light-emitting diodes (LEDs).^{1,2} Among the various ZnO-based TCO films, *n*-ZnO, Al-doped ZnO, and Ga-doped ZnO (GZO) are very attractive materials for the Ohmic contacts on LEDs because they are highly transparent in the visible region, and are nontoxic.³⁻⁵ $\text{Mg}_x\text{Zn}_{1-x}\text{O}$ alloy, another potential transparent conductive material, has been proposed and widely investigated because MgO has a wider band gap of 7.8 eV than ZnO and mixes well with ZnO. By alloying with dielectric MgO, $\text{Mg}_x\text{Zn}_{1-x}\text{O}$ compounds can be formed with band gaps spanning from 3.4 to 7.8 eV. Moreover, the fabrication of $\text{Mg}_x\text{Zn}_{1-x}\text{O}$ films to widen the usable wavelength range and improve the efficiency of quantum confinement structures is important from the viewpoint of band gap engineering.⁶⁻⁸

Several methods have been utilized to deposit $\text{Mg}_x\text{Zn}_{1-x}\text{O}$ alloys, including pulsed laser deposition,⁹ molecular beam epitaxy,¹⁰ and radio-frequency (rf) magnetron sputtering.¹¹ However, few studies report the influence of rapid thermal cycling on rf magnetron sputter deposited $\text{Mg}_x\text{Zn}_{1-x}\text{O}$ films. Therefore, this study analyzes $\text{Mg}_x\text{Zn}_{1-x}\text{O}$ films, which were deposited on a sapphire substrate by rf magnetron sputtering system at room temperature with subsequent annealing at 500, 600, 700, and 800 °C for 60 s in nitrogen ambient. This

study also presents the temperature sensitivities of the electric and optical characterizations of $\text{Mg}_x\text{Zn}_{1-x}\text{O}$ films. The Hall measurement was used to characterize the $\text{Mg}_x\text{Zn}_{1-x}\text{O}$ films. The composition of the $\text{Mg}_x\text{Zn}_{1-x}\text{O}$ films was analyzed by x-ray photoelectron spectroscopy (XPS) and x-ray diffraction (XRD). Transmission spectra were also measured to investigate the optical properties of $\text{Mg}_x\text{Zn}_{1-x}\text{O}$ films.

II. EXPERIMENT

All the $\text{Mg}_x\text{Zn}_{1-x}\text{O}$ films used in this study were grown at room temperature by the rf sputtering method on *c*-face sapphire substrates. The $\text{Mg}_x\text{Zn}_{1-x}\text{O}$ films were formed by a 6 in. ZnO/MgO (80/20 wt %) target. Before being loaded into a deposition chamber, the substrates were cleaned in an ultrasonic bath with acetone, isopropyl alcohol, and de-ionized water for 5 min, respectively. The targets were presputtered for 15 min before growth. Sputtering was carried out at an argon flow rate of 9 SCCM (SCCM denotes cubic centimeter per minute at STP), a pressure of 1.2×10^{-3} Torr, and a sputtering power of 150 W. The distance between the target and the substrate was fixed at 7.2 cm. The growth time was 150 min, and the chamber was cooled using a water cooled chiller system during deposition. The thickness of the deposited $\text{Mg}_x\text{Zn}_{1-x}\text{O}$ was 180 nm, as measured by a Veeco/Dektak 6M profiler. The $\text{Mg}_x\text{Zn}_{1-x}\text{O}$ samples were then annealed at 500, 600, 700, and 800 °C for 60 s in nitrogen ambient, respectively, in a rapid thermal annealing (RTA) system.

^{a)}Electronic mail: kphsueh@alumni.ncu.edu.tw

TABLE I. Summary of the Hall measurement on the $\text{Mg}_x\text{Zn}_{1-x}\text{O}$ samples annealed at different temperatures.

Temperature	Sheet resistivity (Ω/sq)	Mobility ($\text{cm}^2/\text{V s}$)	Concentration ($1/\text{cm}^3$)
As deposited	N.A.	N.A.	N.A.
500 °C/ $\text{N}_2/60$ s (RTA 500 °C)	N.A.	N.A.	N.A.
600 °C/ $\text{N}_2/60$ s (RTA 600 °C)	4.96×10^6	0.22	9.75×10^{17}
700 °C/ $\text{N}_2/60$ s (RTA 700 °C)	2.08×10^5	1.72	2.90×10^{18}
800 °C/ $\text{N}_2/60$ s (RTA 800 °C)	5.55×10^4	5.04	3.72×10^{18}

III. RESULTS AND DISCUSSION

Table I shows the dependence of carrier concentration, electrical resistivity, and Hall mobility of $\text{Mg}_x\text{Zn}_{1-x}\text{O}$ films on the annealing temperatures. The as-deposited and 500 °C-annealed $\text{Mg}_x\text{Zn}_{1-x}\text{O}$ films did not show the Hall results due to high resistivity. However, increasing the annealing temperature decreased resistivity. The lowest resistivity of $5.55 \times 10^4 \Omega \text{ cm}$ associated with the highest mobility and concentration was obtained after 800 °C annealing. Sheu *et al.*¹² reported that the decrease in resistivity that accompanies an increase in annealing temperature could be attributed to an increase in mobility and the carrier concentration, thus reflecting film qualities and the dopants, respectively. In this study, high-temperature annealing should increase the oxygen vacancies in $\text{Mg}_x\text{Zn}_{1-x}\text{O}$ films that play the role of donor, causing an increase in conductivity. Improving the crystallization of $\text{Mg}_x\text{Zn}_{1-x}\text{O}$ films through thermal annealing should also increase mobility.^{12,13}

Figure 1 shows the XRD patterns of $\text{Mg}_x\text{Zn}_{1-x}\text{O}$ samples before and after rapid thermal annealing. Based on the diffraction peaks of ZnO (111) and MgO (111), which are 36.326° and 36.888° , respectively, the pattern of as-grown $\text{Mg}_x\text{Zn}_{1-x}\text{O}$ film shows a strong $\text{Mg}_x\text{Zn}_{1-x}\text{O}$ (111) diffraction peak of 36.21° coupled with a slight MgO_2 (200) diffraction peak of 37.46° . There was a systematic shift of the $\text{Mg}_x\text{Zn}_{1-x}\text{O}$ (111) peak toward a higher diffraction angle as the annealing temperature increased, indicating that the

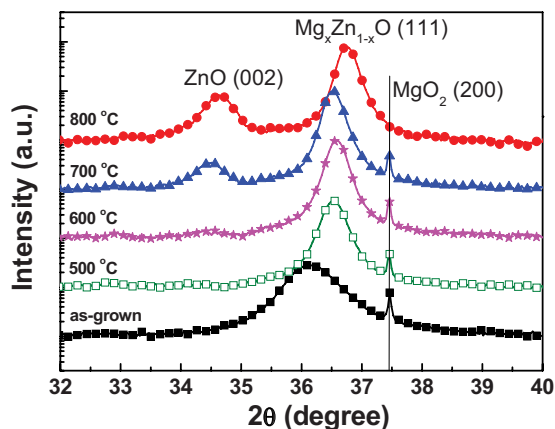


FIG. 1. (Color online) XRD results of as-grown and annealed $\text{Mg}_x\text{Zn}_{1-x}\text{O}$ films deposited on sapphire substrates.

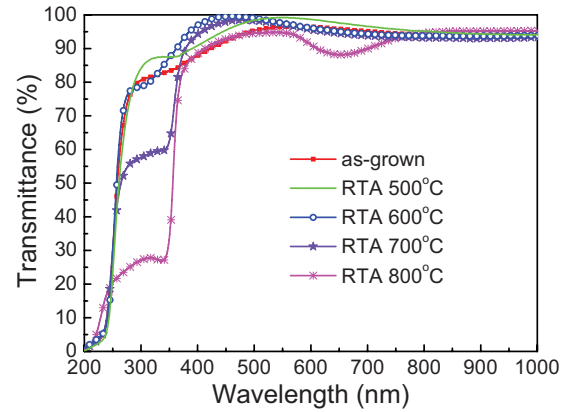


FIG. 2. (Color online) Typical transmission spectra of as-grown and annealed $\text{Mg}_x\text{Zn}_{1-x}\text{O}$ films deposited on sapphire substrates.

strain of the $\text{Mg}_x\text{Zn}_{1-x}\text{O}$ films could be relaxed by thermal annealing. Additionally, the ZnO (002) peak appeared obviously at annealing temperatures of 700 and 800 °C. This suggests that the appearance of only (111) peaks for as-grown film and $\text{Mg}_x\text{Zn}_{1-x}\text{O}$ films annealed at 500 and 600 °C indicates the cubic single phase, whereas the appearance of ZnO (002) peaks in $\text{Mg}_x\text{Zn}_{1-x}\text{O}$ films annealed at 700 and 800 °C confirms the formation of a wurtzite single-phase crystal. The existence of a weak (002)-wurtzite peak besides the (111)-cubic peak indicates the coexistence of two phases after higher thermal annealing.

Figure 2 shows the transmittance spectra of $\text{Mg}_x\text{Zn}_{1-x}\text{O}$ films. In this study, the as-grown $\text{Mg}_x\text{Zn}_{1-x}\text{O}$ film showed high transparency with transmittances over 90% in the visible region (400–700 nm) and the sharp absorption edge was visible in the UV region due to the Mg content. Compared with a previous report about ZnO and GZO films,¹² the absorption edges of these as-grown $\text{Mg}_x\text{Zn}_{1-x}\text{O}$ films shifted toward the short wavelength of 261 nm under 50% transmittances, implying that band gaps can be tuned by changing the Mg content of the $\text{Mg}_x\text{Zn}_{1-x}\text{O}$ layer. The absorption edges of annealed $\text{Mg}_x\text{Zn}_{1-x}\text{O}$ films changed slightly at 500 and 600 °C. However, the absorption spectra of $\text{Mg}_x\text{Zn}_{1-x}\text{O}$ films annealed at 700 and 800 °C showed two stages at wavelengths of 357 and 261 nm. These results show that the ZnO films were separated from this study, $\text{Mg}_x\text{Zn}_{1-x}\text{O}$ films after higher thermal annealing. Additionally, the composition of ZnO (002) film in $\text{Mg}_x\text{Zn}_{1-x}\text{O}$ films increases as the thermal annealing temperature increased, which is consistent with the XRD results.

XPS analysis was used to analyze the composition of the as-grown and annealed $\text{Mg}_x\text{Zn}_{1-x}\text{O}$ films, and the binding energies were calibrated using the carbon (C 1s) peak (285.0 eV) as a reference.¹⁴ The XPS analysis was performed by a Thermo VG-Scientific/Sigma Probe instrument. After the XPS analysis of the surface, a depth analysis was also performed. The samples were etched by an Ar ion beam for depth analysis in the same vacuum system. Figure 3 shows the C 1s, O 1s, Zn 2p_{3/2}, and Mg 2p spectra of as-grown $\text{Mg}_x\text{Zn}_{1-x}\text{O}$ film. Figure 3(a) shows that the amount of car-

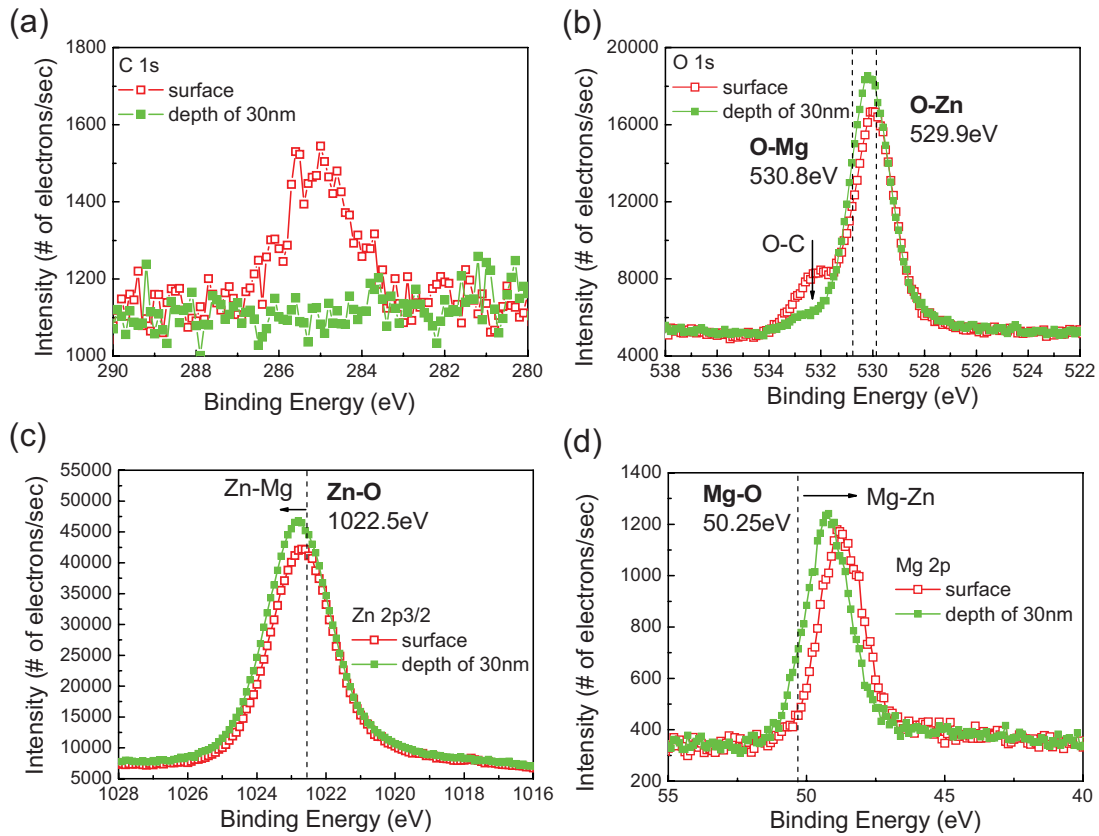


FIG. 3. (Color online) XPS results of (a) C 1s, (b) O 1s, (c) Zn 2p_{3/2}, and (d) Mg 2p spectra of as-grown $Mg_xZn_{1-x}O$ film at the surface and a depth of 30 nm, respectively.

bon contamination was reduced after etching to a depth of 30 nm. Figures 3(b)–3(d) show that, after removing the surface contamination of carbon, the O 1s intensity of the O–C binding energy decreased but the O 1s intensity of the O–Zn and O–Mg binding energies, the Zn 2p_{3/2} intensity of the Zn–O binding energy, and the Mg 2p intensity of the Mg–O binding energy all increased. At a depth of 30 nm, the binding energy in the O 1s spectrum of the as-grown $Mg_xZn_{1-x}O$ film shifted to the middle of the O–Mg peak (530.8 eV) and O–Zn peak (529.9 eV). The binding energy in the Zn 2p_{3/2} spectrum and the binding energy in the Mg 2p spectrum both shifted to a higher binding state. These results indicate that the valence band states of Mg–O and Zn–O become steady after removing the surface contamination of carbon. Additionally, the Zn 2p_{3/2} peak and Mg 2p peak were not at 1022.5 eV (Zn–O) and 50.25 eV (Mg–O), respectively, due to the added Mg–Zn binding energy.

This study also investigates the thermal effect of XPS spectra on $Mg_xZn_{1-x}O$ films. Figure 4 shows the O 1s spectra of as-grown and annealed at 800 °C $Mg_xZn_{1-x}O$ films at a depth of 30 nm. In Fig. 4, the O 1s signals for $Mg_xZn_{1-x}O$ films containing O are deconvoluted in two overlapping peaks. The peaks at 530.8 and 529.9 eV can reasonably be assigned to O²⁻ in O–Mg and in O–Zn, respectively, based on values reported in literatures.^{15,16} Figures 4(a) and 4(b) show that the as-grown $Mg_xZn_{1-x}O$ film has an O–Zn/O–Mg composite ratio of 3.8, while the $Mg_xZn_{1-x}O$ film annealed at

800 °C has an O–Zn/O–Mg composite ratio of 4. This means that the O–Zn composition increases after the 800 °C thermal annealing. These results are consistent with the XRD and transmission spectra results.

IV. CONCLUSION

This study investigates the thermal effects of $Mg_xZn_{1-x}O$ films. $Mg_xZn_{1-x}O$ films were deposited by a rf magnetron sputtering system using a ZnO/MgO (80/20 wt %) 6 in. target. The Hall results, XRD, transparent performance, and

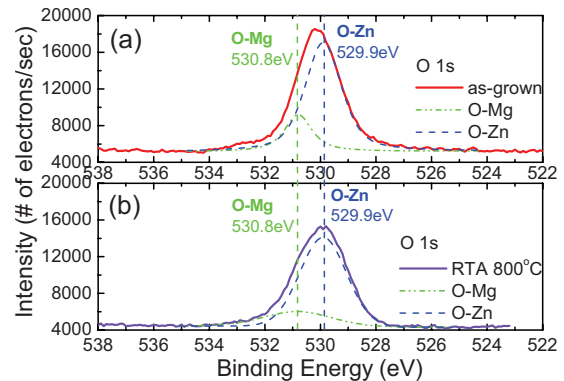


FIG. 4. (Color online) XPS results of O 1s spectrum at a depth of 30 nm. (a) As-grown $Mg_xZn_{1-x}O$ film and (b) the 800 °C annealed $Mg_xZn_{1-x}O$ film.

XPS spectra were also measured. The XRD results indicate that the appearance of only (111) peaks for as-grown Mg_xZn_{1-x}O film indicate the cubic single phase, whereas the appearance of ZnO (002) peaks in Mg_xZn_{1-x}O films annealed at 700 and 800 °C confirms the formation of a wurtzite single-phase crystal. The existence of a weak (002)-wurtzite peak besides the (111)-cubic peak indicates the coexistence of two phases. The absorption spectra of Mg_xZn_{1-x}O annealed at 700 and 800 °C show two stages of transmission spectra at wavelengths of 357 and 261 nm. The XPS spectra of Mg_xZn_{1-x}O films were also demonstrated. The XRD, absorption spectra, and XPS results show that the ZnO films were separated into MgO and ZnO after higher thermal annealing.

ACKNOWLEDGMENTS

The authors would like to thank the National Science Council of Taiwan for financially supporting this research under Contract No. NSC 98-2221-E-238-020. Y. M. Hsin is appreciated for his valuable discussions and technical support.

- ¹J. O. Song, K. K. Kim, S. J. Park, and T. Y. Seong, *Appl. Phys. Lett.* **83**, 479 (2003).
- ²C.-J. Tun, J.-K. Sheu, B.-J. Pong, M.-L. Lee, M.-Y. Lee, C.-K. Hsieh, C.-C. Hu, and G.-C. Chi, *IEEE Photonics Technol. Lett.* **18**, 274 (2006).
- ³C. T. Walsh, H. H. Sandstead, A. S. Prasad, P. M. Newberne, and P. J. Fraker, *Environ. Health Perspect.* **102**, 5 (1994).
- ⁴R. K. Shukla, A. Srivastava, A. Srivastava, and K. C. Dubey, *J. Cryst. Growth* **294**, 427 (2006).
- ⁵T. Minami, *Semicond. Sci. Technol.* **20**, S35 (2005).
- ⁶S. Choojun, R. D. Vispute, W. Yang, R. P. Sharma, T. Venkatesan, and H. Shen, *Appl. Phys. Lett.* **80**, 1529 (2002).
- ⁷W. Yang, R. D. Vispute, S. Choojun, R. P. Sharma, T. Venkatesan, and H. Shen, *Appl. Phys. Lett.* **78**, 2787 (2001).
- ⁸X. Chen, K. Ruan, G. Wu, and D. Bao, *Appl. Phys. Lett.* **93**, 112112 (2008).
- ⁹A. Y. Polyakov, N. B. Smirnov, A. V. Govorkov, E. A. Kozhukhova, A. I. Belogorokhov, H. S. Kim, D. P. Norton, and S. J. Pearton, *J. Appl. Phys.* **103**, 083704 (2008).
- ¹⁰S. Fujita, H. Tanaka, and S. Fujita, *J. Cryst. Growth* **278**, 264 (2005).
- ¹¹Y. Y. Kim, C. H. An, M. K. Cho, J. H. Kim, H. S. Lee, E. S. Jung, and H. S. Kim, *Thin Solid Films* **516**, 5602 (2008).
- ¹²J. K. Sheu, K. W. Shu, M. L. Lee, C. J. Tun, and G. C. Chi, *J. Electrochem. Soc.* **154**, H521 (2007).
- ¹³G. Neumann, *Phys. Status Solidi B* **105**, 605 (1981).
- ¹⁴X. D. Peng and M. A. Barteau, *Surf. Sci.* **224**, 327 (1989).
- ¹⁵J. C. Fuggle, *Surf. Sci.* **69**, 581 (1977).
- ¹⁶B. R. Strohmeier and D. M. Hercules, *J. Catal.* **86**, 266 (1984).